



Breakdown of antiferromagnet order in polycrystalline NiFe/NiO bilayers probed with acoustic emission

M. Lebyodkin, T. Lebedkina, I. Shashkov, V. Gornakov

► To cite this version:

M. Lebyodkin, T. Lebedkina, I. Shashkov, V. Gornakov. Breakdown of antiferromagnet order in polycrystalline NiFe/NiO bilayers probed with acoustic emission. *Applied Physics Letters*, 2017, 111 (3), pp.032407. 10.1063/1.4994812 . hal-02357755

HAL Id: hal-02357755

<https://hal.science/hal-02357755>

Submitted on 10 Nov 2019

HAL is a multi-disciplinary open access archive for the deposit and dissemination of scientific research documents, whether they are published or not. The documents may come from teaching and research institutions in France or abroad, or from public or private research centers.

L'archive ouverte pluridisciplinaire **HAL**, est destinée au dépôt et à la diffusion de documents scientifiques de niveau recherche, publiés ou non, émanant des établissements d'enseignement et de recherche français ou étrangers, des laboratoires publics ou privés.

Breakdown of antiferromagnet order in polycrystalline NiFe/NiO bilayers probed with acoustic emission

M. A. Lebyodkin, T. A. Lebedkina, I. V. Shashkov, and V. S. Gornakov

Citation: *Appl. Phys. Lett.* **111**, 032407 (2017); doi: 10.1063/1.4994812

View online: <http://dx.doi.org/10.1063/1.4994812>

View Table of Contents: <http://aip.scitation.org/toc/apl/111/3>

Published by the [American Institute of Physics](#)



Breakdown of antiferromagnet order in polycrystalline NiFe/NiO bilayers probed with acoustic emission

M. A. Lebyodkin,^{1,a)} T. A. Lebedkina,¹ I. V. Shashkov,² and V. S. Gornakov²

¹Laboratoire d'Etude des Microstructures et de Mécanique des Matériaux, Université de Lorraine, CNRS UMR 7239, Ile du Saulcy, 57045 Metz, France

²Institute of Solid State Physics, Russian Academy of Sciences, 142432 Chernogolovka, Russia

(Received 5 February 2017; accepted 7 July 2017; published online 19 July 2017)

Magnetization reversal of polycrystalline NiFe/NiO bilayers was investigated using magneto-optical indicator film imaging and acoustic emission techniques. Sporadic acoustic signals were detected in a constant magnetic field after the magnetization reversal. It is suggested that they are related to elastic waves excited by sharp shocks in the NiO layer with strong magnetostriction. Their probability depends on the history and number of repetitions of the field cycling, thus testifying the thermal-activation nature of the long-time relaxation of an antiferromagnetic order. These results provide evidence of spontaneous thermally activated switching of the antiferromagnetic order in NiO grains during magnetization reversal in ferromagnet/antiferromagnet (FM/AFM) heterostructures. The respective deformation modes are discussed in terms of the thermal fluctuation aftereffect in the Fulcomer and Charap model which predicts that irreversible breakdown of the original spin orientation can take place in some antiferromagnetic grains with disordered anisotropy axes during magnetization reversal of exchange-coupled FM/AFM structures. The spin reorientation in the saturated state may induce abrupt distortion of isolated metastable grains because of the NiO magnetostriction, leading to excitation of shock waves and formation of plate (or Lamb) waves. *Published by AIP Publishing.* [<http://dx.doi.org/10.1063/1.4994812>]

Ferromagnetic (FM) thin films coupled to antiferromagnetic (AFM) films are characterized by an induced unidirectional (exchange) anisotropy that manifests itself through a shift of the hysteresis loop and enhanced coercivity. The distribution and evolution of spins localized in the antiferromagnet immediately near the FM/AFM interface play a key role in the anisotropy formation.^{1–5} Several models were proposed to explain the shift of the hysteresis loop^{1,2,6–8} and the enhanced coercivity^{9–13} in such heterostructures. Some of them involve the concept of an exchange spin spring (a partial domain wall) twisting/untwisting in the AFM layer during the FM layer reversal from/to the ground state.^{1,4,5,11,14–16} The shift of the hysteresis loop can be explained by reversible switching of FM spins exchange-coupled to spins in the AFM.^{1,2,7} In contrast, the hysteresis loop widening requires irreversible processes.^{8,11–13,16} One suggested mechanism of the coercivity enhancement stems from the spin frustration in the AFM layer,^{2,3} which determines the metastable AFM spin structure at the interface. Several models considered irreversible switching of the AFM order in some polycrystalline grains in the AFM layer during the FM magnetization reversal.^{8,9,11–13,16} More specifically, when the applied field is reversed, a part of spins in the AFM grains is twisted in one way and the others in the other way, leading to the formation of local energy barriers to the reversal.¹⁶ Thermal fluctuations of AFM spins toward the energetically stable state describe the coercivity enhancement in these models.

A system manifesting a strong influence of spin frustration on its irreversible behavior is a FM/AFM heterostructure with a

polycrystalline nickel oxide AFM layer.^{6,14,17–20} Below the Neel temperature, the superexchange coupling between Ni ions contracts the lattice along one of the four $\langle 111 \rangle$ directions in the original cubic unit cell, resulting in a slight rhombohedral deformation of the crystal.²¹ This distortion accompanies the ordering of magnetic moments along one of the $\langle 112 \rangle$ directions in $\{111\}$ planes. It may cause a random easy axis distribution in the NiO layers in either polycrystalline grains^{12,18} or twin domains (T-domains in a single crystal),²⁰ which thus become composed of small regions with one of the four $\langle 111 \rangle$ contraction axes.^{21,22} When the ferromagnetic moment of the FM/AFM bilayer with NiO as the AFM layer is varied, a variation in the local magnetoelastic energy occurs in each region of the NiO film. Sharp coherent AFM spin reorientation in grains during the bilayer switching may lead to a change in their size and, therefore, induce local strains in the AFM layer due to the large NiO magnetostriction.²³ The deviation of the AFM spin structure from its equilibrium configuration during the magnetization reversal in FM/AFM heterostructures leads to a metastable spin rearrangement that is often accompanied by the so-called training effect. It consists of the dependence of the exchange-biased field and coercivity on the field-cycling throughout consecutive hysteresis loops^{24–26} and may be related to the long-time AFM spin relaxation. Since the transformation of the AFM domain structure provides a key to understanding the mechanism of the enhanced coercivity^{8,9,11} and training effect,^{13,24–26} experimental investigations of magnetoelastic properties of FM/AFM heterostructures are of great importance. In the present work, a time-resolved acoustic emission (AE) technique was used to detect ultrasound excitations in the NiO layer during and after the magnetization reversal of the NiFe layer in a NiFe/NiO bilayer.

^{a)} Author to whom correspondence should be addressed: mikhail.lebedkin@univ-lorraine.fr

Polycrystalline NiFe(10 nm)/NiO(50 nm) bilayers of $5 \times 10 \text{ mm}^2$ in size with a mean grain size of approximately 120 \AA were grown by ion beam sputtering onto polycrystalline oxidized silicon substrates. A Permalloy $\text{Ni}_{79}\text{Fe}_{21}$ film was chosen as a ferromagnet layer because it possesses practically zero magnetostriction and magnetocrystalline anisotropy and, consequently, does not contribute to the magnetoelastic response of the NiFe/NiO bilayer. Using permanent magnets producing a 300 Oe uniform bias field in the substrate plane, a unidirectional anisotropy was established in NiFe/NiO during deposition. The macroscopic hysteresis loops of the films were measured at room temperature using a vibrating sample magnetometer in a field parallel to the unidirectional anisotropy axis. The microscopic magnetization reversal processes in the samples were studied using the magneto-optical indicator film (MOIF) technique, which provides real-time information about the domain structure and about defects in the crystal structure, affecting the spin distribution in the sample.^{16,27}

The AE technique used for plasticity studies^{28–30} was adapted to reveal magnetoelastic effects in the films. The specimen was placed within an electromagnet creating the magnetic field up to $H = 1.3 \text{ kOe}$. The AE was captured using a piezoelectric sensor with the operating frequency band in the range of 200–900 kHz, pre-amplified by 60 dB, and recorded at a 2 MHz sampling frequency. The sensor was clamped to the specimen using grease for better contact with the surface. The basics of the method are given in Fig. 1. An abrupt deformation

excites damped elastic waves recorded as a pack of oscillations. Figure 1(a) shows a single AE event (hit) produced by a pencil-lead (Hsu-Nielsen source³¹) break test. Such tests are applied to obtain the impulse response function and verify the acoustic contact between the specimen and the sensor. To avoid damaging the sample, the pencil was broken against the table surface near it. It is seen that the method is sensitive enough to capture acoustic signals from thin films. The impulse response has a rise time about a few microseconds and is damped during several milliseconds. Its Fourier spectrum contains a dominant low-frequency component represented by a large band below approximately 50 kHz [Fig. 1(b)]. Although the interpretation of waveforms related to real deformation processes is sophisticated because of the contribution of the response function, sound reflections, damping properties, and so on, they can provide significant information.^{32,33} In addition, plotting time series of peak amplitudes or durations of hits allows for characterizing the evolution of deformation processes. Figure 1(c) illustrates such a series for noise signals and the pencil-lead test in the absence of magnetic field.

The tests were performed for the in-plane magnetic field oriented either parallel or perpendicular to the unidirectional anisotropy axis. Figure 2 illustrates the results of measurements

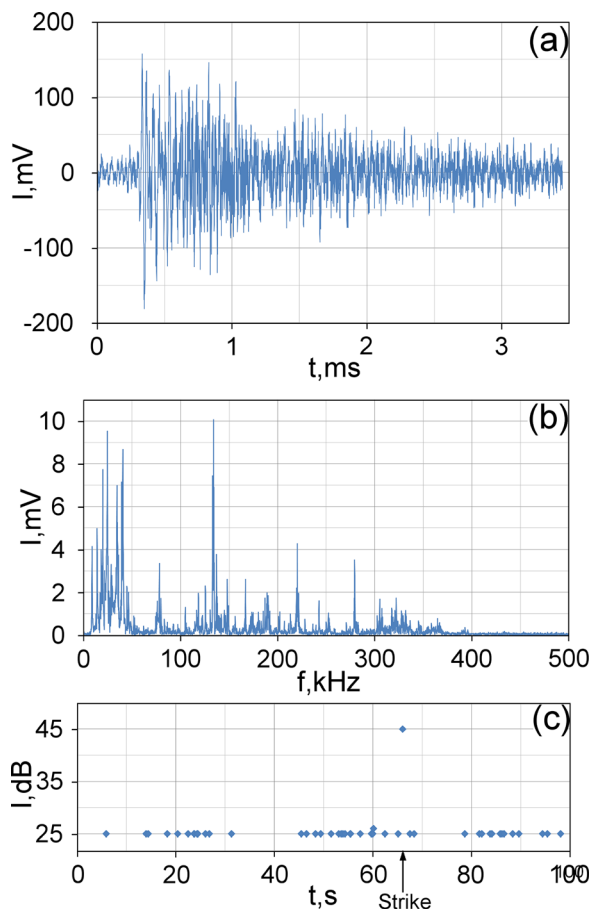


FIG. 1. (a) Acoustic response to an impulse produced by the Hsu-Nielsen source and (b) its Fourier spectrum. The test was performed at the 67th second in the plot (c). Other dots in this plot correspond to noise signals.

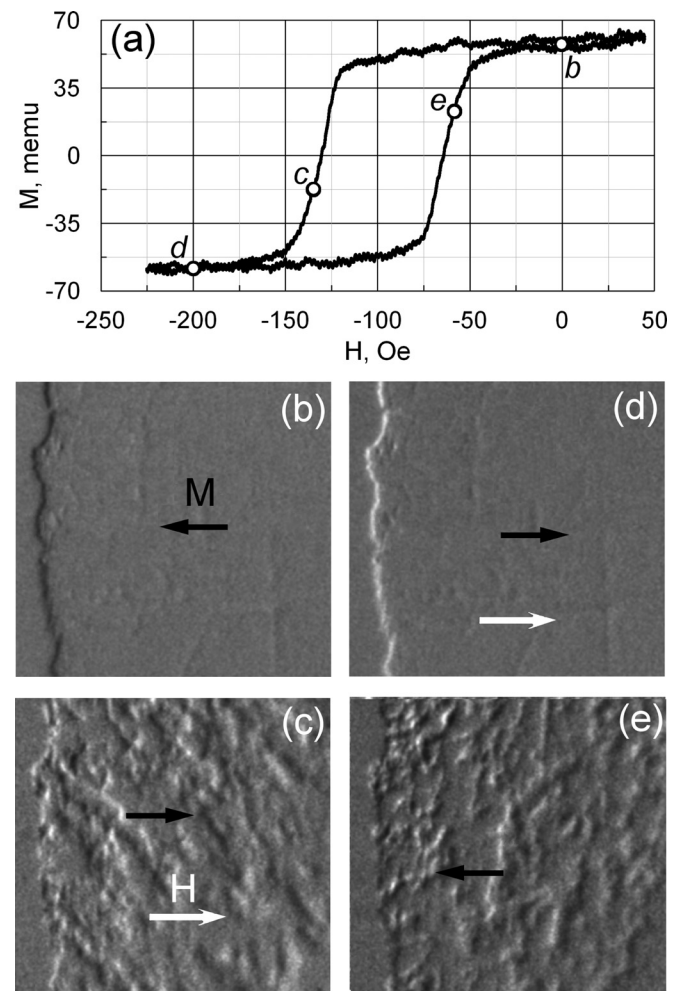


FIG. 2. (a) Hysteresis loop and (b)–(e) MOIF images of the domain structure during magnetization reversal of a polycrystalline NiFe/NiO film in the magnetic field parallel to the unidirectional anisotropy axis. (b)–(e) images correspond to the conditions indicated by the same letters on the hysteresis loop. Black arrows indicate the magnetization directions in the domains.

in a parallel field. The hysteresis loop exhibits an exchange shift ($H_E = 98$ Oe) and substantial coercivity ($H_C = 33$ Oe). The MOIF patterns [Figs. 2(b)–2(e)] of the sample area including its edge (a white or black line on the left side of the image) display the magnetic domain structure of the bilayer. Figures 2(b) and 2(d) show MOIF images of the FM layer in the saturated states at $H = 0$ Oe and $H = 200$ Oe, respectively. In the parallel field, the magnetization reversal both from the ground state [Fig. 2(c)] and to the ground state [Fig. 2(e)] proceeds by nucleation and subsequent growth of small domains with the opposite magnetization orientation. In the perpendicular field, it proceeds by magnetization rotation without domain formation.

Surprisingly, no AE signals were observed during the magnetic field switching with the pulse rise or decay time varied over a wide range from 1 ms to 1 s. In contrast, single acoustic hits were detected in the saturation states at both zero and constant field of either orientation, while waiting for a sufficiently long time. Numerous measurements on several specimens, including variation of the number of the field cycling, its value and orientation, provided the following conclusions, as illustrated in Fig. 3. Series of dots in Figs. 3(a) and 3(b) represent amplitudes of AE events recorded in the parallel and perpendicular fields, respectively, considerably exceeding the noise background indicated by dashed lines. It can be seen that the hit amplitudes and instants of occurrence are scattered randomly after the field switching. The AE events become progressively rarer after the magnetization cycling [cf. Fig. 3(c)], thus testifying the formation of a more stable crystal structure. Figure 3(d) shows that the probability of occurrence of AE decreases down to zero after the magnetization cycling has been stopped. Furthermore, the AE activity depends on the test history. In particular, switching in any order between parallel and perpendicular orientations of the magnetic field resumes the AE activity, as illustrated in Figs. 3(a) and 3(b). It should be specified that MOIF imaging shows no visible net magnetization rotation in the bilayer in the perpendicular field, thus confirming that the AE is observed in the saturated state in both cases.

Similar AE measurements without the bilayer did not reveal any signal above noise. It can thus be concluded that the above-described AE events are caused by elastic waves excited in the NiFe/NiO bilayer. Figure 4 illustrates three typical waveforms and the corresponding Fourier spectra of the recorded hits, one measured at $H = H_d = 200$ Oe [marked as I in Figs. 3(b) and 4] and two others, with different amplitudes, at $H = H_b = 0$ (respectively, II and III). The comparison with Fig. 1 shows that the decay times and the own frequencies differ by an order of magnitude with regard to the pencil-break test. All three spectra given in Fig. 4(b) display similar components, notably, a wide group of high-frequency peaks between 100 kHz and 400 kHz, which are absent in Fig. 1. The low-frequency band dominating in Fig. 1 is negligible in plots II and III of Fig. 4 (zero field conditions) and different in shape in plot I ($H = 200$ Oe). It is noteworthy that the examples obtained in the same conditions (II and III) display very close spectral shapes while the repartition of intensities is somewhat different for the other field orientation. A detailed study of the effect of field orientation will be published elsewhere. The entirety of data testifies that the AE events with different amplitudes recorded in different field conditions, at different instants, and very probably, at different locations, possess similar frequencies. It can thus be suggested that the high-frequency part of Fourier spectra of Fig. 4 reflects the properties of the sound propagation in the investigated media for the given experimental setup, whereas the low-frequency band may characterize the impulse response function of the acoustic probe. The possible nature of the shock processes inside the bilayer, which could initiate the high-frequency oscillations, will be discussed below.

The acoustic sensor detects surface elastic waves with a vertical polarization, i.e., normal to the surface. In the case of thin plates and films, the so-called plate (or Lamb) waves that have such polarization may be excited.^{34–36} Although many specific Lamb wave modes may occur, it is important that the active modes are determined by the film thickness and the material structure, in particular, the elastic anisotropy.³⁶ Therefore,

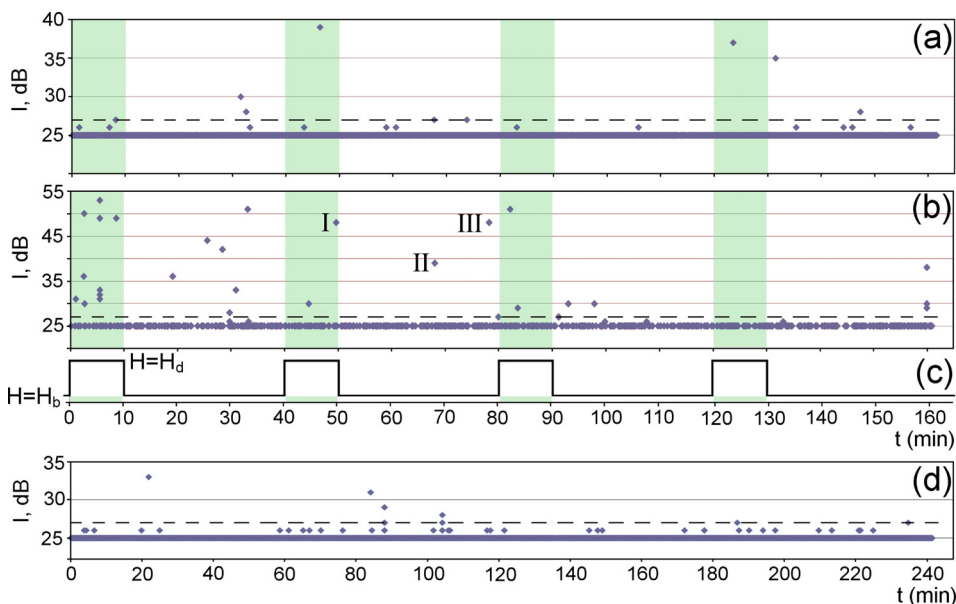


FIG. 3. Acoustic response during a series of switching (a) parallel and (b) perpendicular to the unidirectional anisotropy axis according to the sequence (c). The series (b) immediately followed the sequence (a). Plot (d) demonstrates the decay of AE with time without magnetic field cycling.

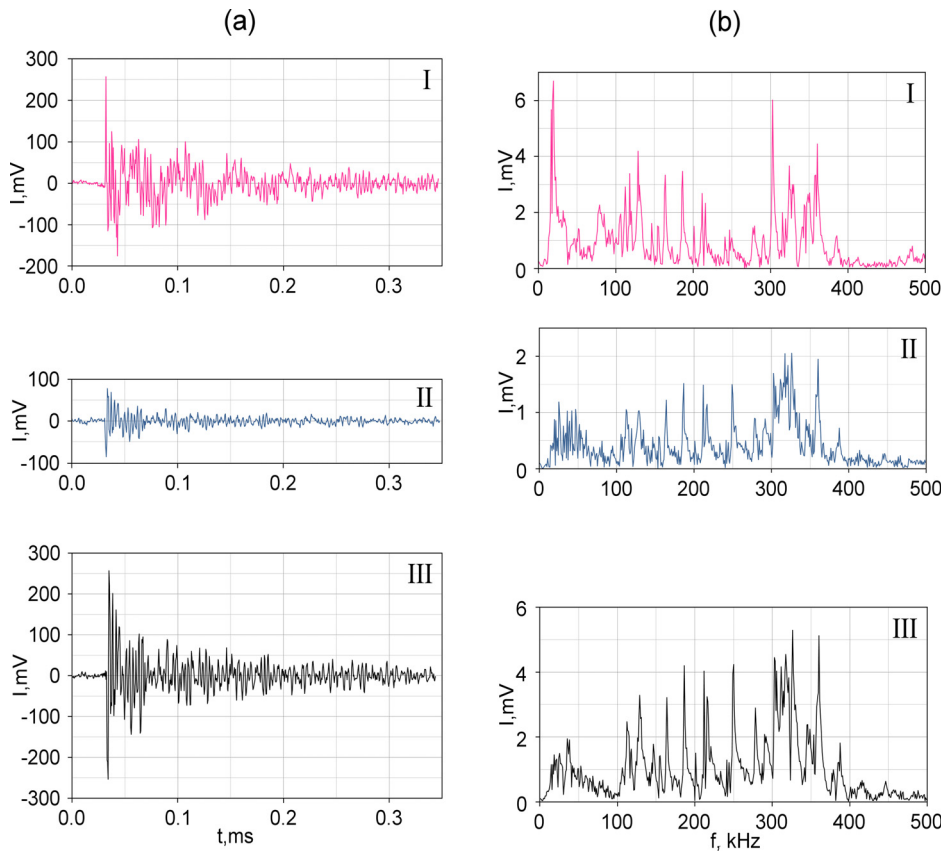


FIG. 4. (a) Waveforms of AE events recorded in the (I) maximum and (II and III) zero magnetic field (see labels in Fig. 3) and (b) the corresponding Fourier spectra.

the persistence of the elastic modes revealed in the Fourier spectra (Fig. 4) suggests the formation of Lamb waves.

Taking into account negligible magnetostriction in NiFe, excitation of elastic oscillations should be attributed to spin rotations in the NiO layer, which are determined by the spin rotations in the NiFe layer through exchange coupling. The following mechanism can be suggested. The nucleation of domains and motion of the domain walls in the bilayer [Figs. 2(b)–2(e)] produce inhomogeneous smooth spin rotation in both FM and AFM layers near the interface.^{1,12,16,25} Due to variation of anisotropy axes in the AFM grains, the coherent FM spin rotation in the magnetic field is accompanied by the generation of small-scale AFM spin spirals in these grains with a right- or left-handed twisting of spins, forming energy barriers for the heterostructure relaxation. The existence of opposite spin chiralities in AFM grains was experimentally confirmed for NiFe/NiO¹² and NiFe/FeMn⁵ exchange-coupled bilayers. The presence of barriers can result in irreversible transitions between two degenerate states of AFM grains^{9,11,13} and excitation of elastic waves because of the magnetostriction. Importantly, such processes must be governed by thermal activation, in agreement with the observed dependences on the time, history, and number of repetitions of the field cycling (cf. Ref. 37).

In the framework of this conjecture, the fact that AE is not observed during the stage of the magnetization reversal may be due to compensation of the effects from different grains in the polycrystalline NiO with a random distribution of easy axes. More precisely, the magnetic moments are rotated both clockwise and counterclockwise in various grains during the magnetization reversal of the FM layer. As a result, magnetoelastic interactions related to different

orientations are statistically compensated and do not generate a magnetostrictive response in the AFM layer.

Two specific processes may be envisaged in the framework of the Fulcomer and Charap model.⁹ First, when the effective average angle of some exchange springs in the anti-ferromagnet exceeds the critical value,¹¹ AFM grains perform a transition to the other state by overcoming the barriers. The energy lost and the respective hysteretic effect result from the irreversible switch of the AFM order in the grains. Some high enough energy barriers may not be overcome during switching or immediately after saturation. The sample will thus reside in a metastable state with energy determined by the twisted grains. The return to the stable state will require thermally activated untwisting processes that can be realized through nucleation and motion of T -domain walls. Both this motion and spin rotation in NiO grains can result in reorientation of the deformation axis and, consequently, magnetostriction. The sharp change in the grain size induced by the magnetostriction in isolated grains undergoing spin reorientation will give rise to a shock wave, which may excite the observed Lamb waves.

The second possible mechanism of elastic waves excitation is a pair recombination process of T -walls in twisted AFM grains.²² T -walls can be easily generated, moved, and annihilated when some grains undergoing deformation because of rotation of their spins produce a nonuniform pressure along $\langle 111 \rangle$ axes in the neighboring grains. The elastic energy stored in two walls might be released during their recombination in the form of elastic shear wave pulse which will propagate along the NiO layer as Lamb waves. In particular, excitation of such pulses during recombination of pairs of T -walls could be the reason of the twinning “cry” in NiO crystals reported by Slack.²¹

In summary, the acoustic response was studied during and after in-plane magnetization reversal in exchange-biased polycrystalline NiFe/NiO bilayers. Sporadic AE events were detected in the constant magnetic field corresponding to full saturation of the FM layer. The AE is interpreted as the surface Lamb waves excited by sharp shocks in the NiO layer. The observed phenomenon is discussed in the framework of the model of the thermal fluctuation aftereffect in the exchange-coupled FM/AFM structures.⁹ It considers the irreversible breakdown of the original spin orientation in AFM grains with disordered anisotropy axes during the magnetization reversal in the FM/AFM system. The presented results thus provide evidence of spontaneous thermally activated switching of the AFM order in NiO grains in a FM/AFM heterostructure. Unresolved by optical imaging or magnetization measurements, these processes occur to give rise to measurable acoustic signals, due to a strong magnetostriction of NiO.

V.G. and I.Sh. acknowledge support from the Université de Lorraine for one month visits to LEM3. I.Sh. acknowledge support from RFBR (Grant No. 16-32-00264). T.L. acknowledges support by the Region Lorraine (France) and the Center of Excellence “LabEx DAMAS” (Grant No. ANR-11-LABX-0008-01 of the French National Research Agency).

- ¹D. Mauri, H. C. Siegmann, P. S. Bagus, and E. Kay, *J. Appl. Phys.* **62**, 3047 (1987).
- ²A. P. Malozemoff, *Phys. Rev. B* **35**, 3679 (1987).
- ³A. I. Morosov and A. S. Sigov, *Phys. Solid State* **46**, 395 (2004).
- ⁴A. Scholl, M. Liberati, E. Arenholz, H. Ohldag, and J. Stöhr, *Phys. Rev. Lett.* **92**, 247201 (2004).
- ⁵C. L. Chien, V. S. Gornakov, V. I. Nikitenko, A. J. Shapiro, and R. D. Shull, *Phys. Rev. B* **68**, 014418 (2003).
- ⁶J. Nogues, J. Sort, V. Langlais, V. Skumryev, S. Suriñach, J. S. Muñoz, and M. D. Baró, *Phys. Rep.* **422**, 65 (2005).
- ⁷F. Radu and H. Zabel, *Tracts Mod. Phys.* **227**, 97 (2008).
- ⁸M. D. Stiles and R. D. McMichael, *Phys. Rev. B* **59**, 3722 (1999).
- ⁹E. Fulcomer and S. H. Charap, *J. Appl. Phys.* **43**, 4190 (1972).
- ¹⁰T. C. Schulthess and W. H. Butler, *Phys. Rev. Lett.* **81**, 4516 (1998).
- ¹¹M. D. Stiles and R. D. McMichael, *Phys. Rev. B* **63**, 064405 (2001).

- ¹²T. Zhao, H. Fujiwara, K. Zhang, C. Hou, and T. Kai, *Phys. Rev. B* **65**, 014431 (2001).
- ¹³H. Xi, R. M. White, S. Mao, Z. Gao, Z. Yang, and E. Murdock, *Phys. Rev. B* **64**, 184416 (2001).
- ¹⁴V. I. Nikitenko, V. S. Gornakov, L. M. Dedukh, Yu. P. Kabanov, A. F. Khapikov, A. J. Shapiro, R. D. Shull, A. Chaiken, and R. P. Michel, *Phys. Rev. B* **57**, R8111 (1998).
- ¹⁵V. I. Nikitenko, V. S. Gornakov, A. J. Shapiro, R. D. Shull, K. Liu, S. M. Zhou, and C. L. Chien, *Phys. Rev. Lett.* **84**, 765 (2000).
- ¹⁶V. S. Gornakov, Yu. P. Kabanov, O. A. Tikhomirov, V. I. Nikitenko, S. V. Urzhidn, F. Y. Yang, C. L. Chien, A. J. Shapiro, and R. D. Shull, *Phys. Rev. B* **73**, 184428 (2006).
- ¹⁷R. P. Michel, A. Chaiken, C. T. Wang, and L. E. Johnson, *Phys. Rev. B* **58**, 8566 (1998).
- ¹⁸J. McCord, R. Kaltofen, T. Gemming, R. Hühne, and L. Schultz, *Phys. Rev. B* **75**, 134418 (2007).
- ¹⁹W. Zhu, L. Seve, R. Sears, B. Sinkovic, and S. S. P. Parkin, *Phys. Rev. Lett.* **86**, 5389 (2001).
- ²⁰H. Ohldag, A. Scholl, F. Nolting, S. Anders, F. U. Hillebrecht, and J. Stöhr, *Phys. Rev. Lett.* **86**, 2878 (2001).
- ²¹G. A. Slack, *J. Appl. Phys.* **31**, 1571 (1960).
- ²²W. L. Roth, *J. Appl. Phys.* **31**, 2000 (1960).
- ²³T. R. McGuire and W. A. Crapo, *J. Appl. Phys.* **33**, 1291 (1962).
- ²⁴X. Portier, A. K. Petford-Long, A. de Morais, N. W. Owen, H. Laidler, and K. O'Grady, *J. Appl. Phys.* **87**, 6412 (2000).
- ²⁵A. N. Dobrynin, F. Maccherozzi, S. S. Dhesi, R. Fan, P. Bencok, and P. Steadman, *Appl. Phys. Lett.* **105**, 032407 (2014).
- ²⁶Z. Tian, C. Zhu, Y. Liu, J. Shi, Z. Ouyang, Z. Xia, G. Du, and S. Yuan, *J. Appl. Phys.* **115**, 083902 (2014).
- ²⁷L. H. Bennett, R. D. McMichael, L. J. Swartzendruber, S. Hua, D. S. Lashmore, A. J. Shapiro, V. S. Gornakov, L. M. Dedukh, and V. I. Nikitenko, *Appl. Phys. Lett.* **66**, 888 (1995).
- ²⁸M. A. Lebyodkin, N. P. Kobelev, Y. Bougherira, D. Entemeyer, C. Fressengeas, V. S. Gornakov, T. A. Lebedkina, and I. V. Shashkov, *Acta Mater.* **60**, 3729 (2012).
- ²⁹I. V. Shashkov, M. A. Lebyodkin, and T. A. Lebedkina, *Acta Mater.* **60**, 6842 (2012).
- ³⁰M. A. Lebyodkin, I. V. Shashkov, T. A. Lebedkina, and V. S. Gornakov, *Phys. Rev. E* **95**, 032910 (2017).
- ³¹N. N. Hsu and F. R. Breckenridge, *Mater. Eval.* **39**, 60 (1981).
- ³²A. Vinogradov, D. L. Merson, V. Patlan, and S. Hashimoto, *Mater. Sci. Eng., A* **341**, 57 (2003).
- ³³M. A. Lebyodkin, T. A. Lebedkina, F. Chmelík, T. T. Lamark, Y. Estrin, C. Fressengeas, and J. Weiss, *Phys. Rev. B* **79**, 174114 (2009).
- ³⁴H. Lamb, *Proc. R. Soc. London, Ser. A* **93**, 114 (1917).
- ³⁵I. A. Viktorov, *Rayleigh and Lamb Waves: Physical Theory and Applications* (Plenum Press, New York, USA, 1967).
- ³⁶S. V. Kuznetsov, *Acoust. Phys.* **60**, 95 (2014).
- ³⁷A. Planes, F.-J. Pérez-Reche, E. Vives, and L. Mañosa, *Scr. Mater.* **50**, 181 (2004).